Available online at www.sciencedirect.com
ScienceDirect
Polymer 48 (2007) 3237–3247
polymer
www.elsevier.com/locate/polymer

Molecular assembled self-doped polyaniline copolymer ultra-thin films

Chien-Hsin Yang [a,*], Liang-Ren Huang [b], Yi-Kai Chih [c], Wen-Churng Lin [d], Feng-Jiin Liu [e], Tzong-Liu Wang [a]

[a] *Department of Chemical and Materials Engineering, National University of Kaohsiung, Kaohsiung 811, Taiwan*
[b] *Department of Chemical and Materials Engineering, Southern Taiwan University of Technology, Tainan 710, Taiwan*
[c] *Department of Chemical Engineering, National Cheng-Kung University, Tainan 701, Taiwan*
[d] *Department of Environmental Engineering, Kun-Shan University, Tainan 710, Taiwan*
[e] *Department of Chemical Engineering, National United University, Miaoli 360, Taiwan*

Received 28 October 2006; received in revised form 17 March 2007; accepted 3 April 2007
Available online 19 April 2007

Abstract

A self-assembly technique and copolymerization were used to buildup a self-doped polyaniline (SPANI) ultra-thin film on an indium-tin oxide (ITO) substrate. The monomers used were aniline and its derivative MSAN (*m*-aminobenzenesulfonic acid). Successful MSAN/AN copolymerization and film formation were simultaneously performed in aqueous solution with the addition of oxidant (APS, ammonium persulfate). The film deposition rate of a high AN/MSAN ratio system is generally higher than that of a low AN/MSAN ratio system. Cyclic voltammetry, UV–vis spectroscopy, and α-step instruments indicate a systematic dependence of the film thickness of these ultra-thin films on the assembly time and temperatures. The Auger depth profile reveals the elemental distribution in these films and exhibits different deposition rates between AN and MSAN. XPS N_{1s} spectra also show the variation of the degree of doping. This SPANI film can be used as an electrochromic electrode in a corresponding device. Carboxyl-terminated-butadiene-acrylonitrile (CTBN) blended with $LiClO_4$ was used as a solid polymer electrolyte. A total solid electrochromic device was assembled as ITO/SPANI/$LiClO_4$–CTBN/PEDOT:PSS/ITO, where PEDOT:PSS is poly(3,4-ethylenedioxythiophene)/poly(4-styrenesulfonate) as the counter complementary electrode. The device was pale gray at −1.5 V and blue at +1.5 V.

Keywords: Self-doped polyaniline (SPANI); Molecular self-assembly; Ultra-thin film

1. Introduction

Conducting polymer is a promising material for further applications in molecular electronics, molecular wires, and devices [1,2]. Polyaniline (PANI) is the simplest linear conjugated macromolecule and a representative of conducting polymers [3]. To combine two or more desirable properties, multicomposites can provide additional stability for molecular assembly. Even fine device functionality will result from a combination of physical and chemical processes (e.g., electron and energy transfer). Such a device requires control of molecular orientation and organization on the nanoscale, because its function significantly depends on the local chemical environment. Therefore, scientists greatly desire to develop methods for the controllable assembly of multicomponent nanostructures.

Single molecular layers can be consecutively deposited onto planar solid supports and then form multilayers in which organic molecules can be controlled in at least one dimension with nanoscale arrangements. This process clarifies a fixed relation between nanoscopic order and macroscopic orientation to develop functional macroscopic devices. To fully exploit an assembled structure, it is necessary to know the location or orientation of the molecules [4]. In these systems, the molecularly controlled fabrication of monolayer films has been

* Corresponding author. Tel.: +886 7 5919420; fax: +886 6 2425741.
E-mail address: yangch@nuk.edu.tw (C.-H. Yang).

0032-3861/$ - see front matter © 2007 Elsevier Ltd. All rights reserved.
doi:10.1016/j.polymer.2007.04.013

dominated by the Langmuir–Blodgett (LB) technique [5]. Monolayers are formed on a water surface and then transferred onto a solid support. The LB technique requires special equipment and has severe limitations in substrate size and topology as well as in film quality and stability. Since 1980s, self-assembly techniques have been developed as an alternative to LB films in a silane–SiO_2 interface [6], metal phosphonate chemistry [7], as well as ultra-thin films of Zener diodes from conducting polymers and CdSe nanoparticles [8]. Based on covalent and coordination chemistry, self-assembled films are restricted to certain classes of organics, and high-quality multilayer films cannot be reliably obtained. These problems mainly arise from the high steric demand of covalent chemistry, which is a prerequisite for remaining functional group density in each layer.

Recently, the layer-by-layer polyelectrolyte (such as polyanion and polycation) deposition route has been developed for the fabrication of ultra-thin polymer layers [9–11]. Using this route, the incorporation of ultra-thin (<100 Å) charge-injection interfacial layers in polymer light-emitting diodes [12] has been achieved. Polycations and polyanions are alternately adsorbed from their respective solutions onto the substrate to form a multilayer film in which the thickness and other physico-chemical properties of the sub-layers can be tuned over molecular widths [9–12]. A strong cooperative ion-pair interaction locks the chain segments into highly interpenetrated structures [9–12] to buildup a multilayer film at the molecular level. Here we fabricated the thin film of self-doped polyaniline on an indium-tin oxide (ITO) substrate. It was desirable to create a simple approach that would form uniform nanoarchitecture films, whereas the fabrication was expected to be independent of the nature, size, and topology of the substrate. The electrostatic attraction between oppositely charged molecules (such as propagating molecule chains) seemed to be a good candidate as a driving force for film buildup, because it possesses the least steric requirement of all chemical bonds. Strong electrostatic attraction occurs between a charged surface and oppositely charged molecule in solution. This phenomenon has been known for the adsorption of small organics and polyelectrolytes [13], but it has rarely been studied with respect to the film formation of propagating conducting polymers. The formation of self-doped polyaniline ultra-thin films has important consequences for flocculation and is therefore of interest in large-scale processes such as charge-injection layers in polymer light-emitting diodes [12] and electrode materials in electrochromic device [2]. However, this process is considered to be an alternative method to fabricate uniform thin films. These applications may benefit from a better understanding of self-doped polyaniline films as model systems, as these can be well characterized by a wide variety of physical techniques.

In this work, aniline (AN) was dissolved in an aqueous solution of *m*-aminobenzenesulfonic acid (MSAN). MSAN was used as a monomer, a surfactant, and a self-dopant. Then, ammonium persulfate (APS) was added as the oxidant. A series of ultra-thin films were visually observed during the assembly.

2. Experimental section

2.1. Chemicals

Aniline (Merck) was distilled under reduced pressure. *m*-Aminobenzenesulfonic acid (Acros) was purified by recrystallization two times from distilled water using the method of our previous work [14]. Oxidants (ammonium peroxydisulfate (APS), Wako), lithium perchlorate ($LiClO_4$, Merck), carboxyl-terminated-butadiene-acrylonitrile (CTBN, Hycar 1300× 8), and poly(3,4-ethylenedioxythiophene) (PEDOT)–poly(4-styrenesulfonate) (PSS) (Merck) were used as received. The ITO-coated glass substrates ($\sim 10\ \Omega\,cm^{-2}$, Merck) were first cleaned by a mixture of $H_2O/H_2O_2/NH_3$ with the ratio of 10:2:0.6 at 55–60 °C for 1 h. The substrates were baked in a vacuum (165–170 °C, 150 min) to remove physisorbed water and followed by UV–O_3 irradiation for 20 min.

2.2. Self-assembly of SPANI ultra-thin films

Aniline and MSAN (total $-NH_2$ concentration kept at 0.057 M) were dissolved in 100 mL of distilled water with a desired AN/MSAN mole ratio ranging from 0.25 to 4.0. Far from the intervals, the experiments were difficult to perform. The solution was magnetically stirred at a specific reaction temperature (4–25 °C). An aqueous solution of $(NH_4)_2S_2O_8$ (0.57 g) with a 12.5 mL volume was added to the above monomer mixture in one portion at the same temperature. The resulting solution was stirred for another 2 min to ensure complete mixing. To develop a film of SPANI as illustrated schematically in Fig. 1, SPANI-based ultra-thin

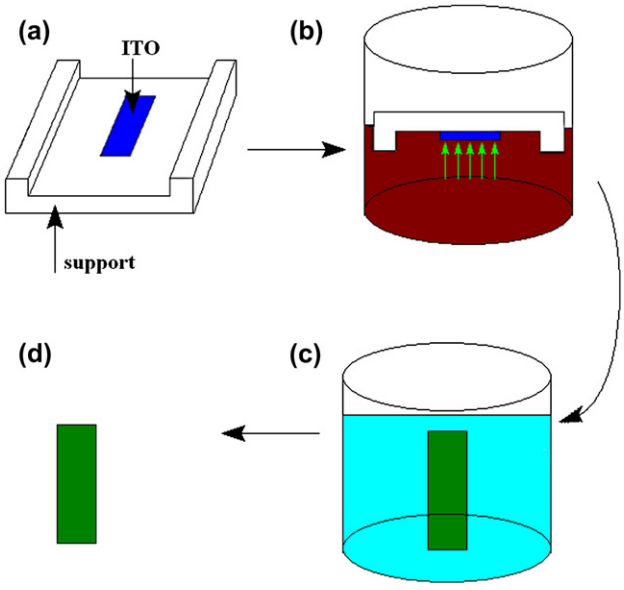

Fig. 1. Schematic of the SPANI film deposition process employed an immersing self-assembly method. Step a represents the fixing of the ITO glass onto a support. Step b is the deposition of a SPANI film in the reaction solution, and steps c and d are washing and drying steps, respectively. The four steps are the basic buildup sequence for an ultra-thin film of SPANI. Chemical components in the reaction solution have aniline, *m*-aminobenzenesulfonic acid, ammonium peroxydisulfate, and water.

films were assembled on ITO glass using a combined self-assembly and copolymerization method at a fixed temperature in the range of 4–25 °C. Far from the intervals, the experiments could not be smoothly performed. After that, the resulting films were taken from the reaction solution and washed several times with dry acetonitrile in a glove box purging argon. Finally, this film was dried in a dynamic vacuum at room temperature for 24 h. This process, which is extremely simple, is depicted in Fig. 1, for the case of self-doped polyaniline deposition on a charged surface (ITO).

2.3. Characterization of SPANI films

This assembled a conformed layer in the form of a dense stack. The thickness was determined by α-step method (Surfocorder TE 2400 M, Tosaka Lab. Ltd.). The formed SPANI films on ITO were analyzed by a UV–vis spectrophotometer (Lambda 25 diode-array spectrometer, Perkin–Elmer). Cyclic voltammetric (CV) measurements were performed in 0.1 M $LiClO_4$/propylene carbonate (PC) solution using a PGSTAT 20 electrochemical analyzer (AUTOLAB Electrochemical Instrument, The Netherlands). Scanning electron microscopy (SEM) was performed on a Philips apparatus (XL-40 FEG), which was operated at low acceleration voltage ($V_{acc} = 15$ kV) to minimize charging of the as-synthesized samples. Micelle morphology in a freeze-fracture replica sample taking in the reaction solution was observed by a transmission electron microscope (TEM, JEM-1230, JEOL Ltd., Japan) with an acceleration voltage of 80 kV. Auger electron spectroscopic (AES) measurements were performed with a MICROLAB 310D spectrometer (VG Scientific Ltd.). AES depth profiling was performed at emission currents of 0.1 and 8 mA with gun tensions of 10 (electron) and 3 kV (ion), respectively. Sputtering velocity was set at 1 Å s^{-1}. The X-ray photoelectron spectroscopic (XPS) measurements were performed with ESCA 210 and MICROLAB 310D (VG Scientific Ltd.) spectrometers. XPS spectra were recorded with Mg Kα ($h\nu = 1253.6$ eV) irradiation as the photon source with a primary tension of 12 kV and an emission current of 20 mA. Analysis chamber pressure during the scans was kept at approximately 10^{-10} mbar.

2.4. Preparation of electrolyte in electrochromic device

CTBN of 20 g in methylethylketone (5 wt%) and 10 mL of 0.01 M $LiClO_4$ (Aldrich) in ethanol solution were mixed, and then a thin CTBN–$LiClO_4$ layer was spin-coated on the top of the ITO/SPANI film. Solvent was then dried under vacuum for 24 h.

2.5. Assembly of electrochromic device

Using the ITO-coated SPANI, PEDOT:PSS, and CTBN–$LiClO_4$ films an electrochromic device was assembled: ITO/SPANI//CTBN–$LiClO_4$//PEDOT:PSS/ITO. The entire cell structure (6 cm^2 surface area) was sealed with epoxy resin. Cyclic voltammetry and double-potential chronoamperometry were done with the assembled cell by use of a PGSTAT 30 electrochemical analyzer (AUTOLAB Electrochemical Instrument, The Netherlands). In situ optical characterization was made using a Perkin–Elmer (Lambda 25) UV–vis spectrophotometer in the UV–vis region.

3. Results and discussion

3.1. Self-assembly of SPANI ultra-thin films

To assemble a stable SPANI ultra-thin film on the ITO substrate, the ITO-coated glass was immersed into the reaction solution of AN/MSAN mixture. MSAN is used as a surfactant, a dopant, and a monomer, which coupled with aniline to form micelles in aqueous solution (Fig. 2); whereas aniline may exist in the form of anilinium cations or aniline in the reaction solution. Anilinium cations can be dissolved in the micelle–water interface to form a micelle; a part of AN diffuses into the micelles [14]. The surface of RCA-treated ($H_2O/H_2O_2/NH_3$ used in this work) ITO is basic presumably due to the presence of indium oxide, In_2O_3 (ca. 91%) [15], and is characterized by its availability of surface hydroxyl functionality [16]. This may lead to a preferential adsorption of AN molecules than MSAN molecules at the initial stage of self-assembly. The AN molecules might readily form the hydrogen bonding with ITO substrate. The MSAN molecules possess the property of molecular self-doping, which would retard the formation of hydrogen bonding between MSAN species and ITO substrate. Micelles were regarded as the precursors to further produce SPANI film at the addition of the oxidant (APS), with the polymerization initially performed on the surface of the micelles. With the polymerization proceeding, the micelles thus tend to join along the direction of the polymer chain. The polymer chain acted like a molecular template that adsorbed

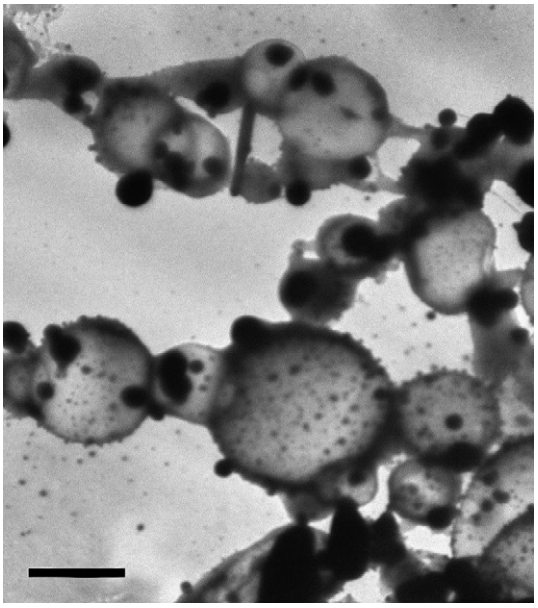

Fig. 2. TEM image of a freeze-fracture replica sample taken from the reaction solution with AN/MSAN mole ratio of 0.25. Scale bar is 1 μm.

on the surface of ITO with the hydrogen bonding between polymer chains and ITO in this self-assembly process. Thus, films are assembled by the micelles through aggregation and fuse to stack an ultra-thin. And, the deposition rate of MSAN-rich systems is lower than that of AN-rich systems. During the polymerization and film assembly, the polymer chains adsorbed on the surface of ITO and then interlocked with the electrostatic force between polaron sites (NH^+) and sulfonate anions ($-SO_3^-$) on the polymer chains. A smooth ultra-thin film could be readily obtained, as the ITO was immersed in the reaction solution to keep 1 cm from the interface of air and reaction solution. The UV–vis absorption spectra of growing SPANI film with AN/MSAN ratio of 0.25 (4 °C) at different assembly times showed three absorption bands (Fig. 3(a)). Referring to the 60 h assembly time, the band at the first maximum absorption wavelength ($\lambda^{I}_{max} = 330$ nm) corresponds to the reduced state (leucoemeraldine) of SPANI. The band at the second maximum absorption wavelength ($\lambda^{II}_{max} = 430$ nm) corresponds to partial oxidation of SPANI and can be assigned to represent the intermediate state between the leucoemeraldine form containing benzenoid rings and the emeraldine form containing conjugated quinoid rings in the backbone of the SPANI. An intermediate state may be attributed to arise by the aggregation of localized radical cations. The emeraldine form transforms into fully oxidized pernigraniline form and characterized by a wide band at around the third maximum absorption wavelength ($\lambda^{III}_{max} = 730$ nm). The three bands would blue shift to lower wavelength upon buildup to thicker film, indicating that the entanglement is more significant among polymer chains with increasing film thickness. Increasing the AN/MSAN ratio to 1 at 4 °C, the UV–vis spectra (Fig. 3(b)) are similar to those in Fig. 3(a). Moreover, the third maximum absorption band of AN/MSAN = 1 shows weaker than that of AN/MSAN = 0.25, suggesting that the low doping level (see later) results in a weak form of the fully oxidized pernigraniline. In reaction solution with AN/MSAN = 0.25 at 15 °C (Fig. 3(c)), a significant blue shift presents above 36 h assembly times. A similar behavior can be observed at reaction temperature of 25 °C. Also note that the results (Fig. 3(d)) of AN/MSAN = 1 are similar to those of AN/MSAN = 0.25 at 15 and 25 °C, respectively. Fig. 4 shows the UV–vis absorbance of SPANI films at $\lambda_{max} = 425$ nm for various assembly times at different reaction temperatures. The absorbance increases with increasing assembly time, indicating that a SPANI film was readily buildup with an increase of time. On the other hand, the absorbance increases with

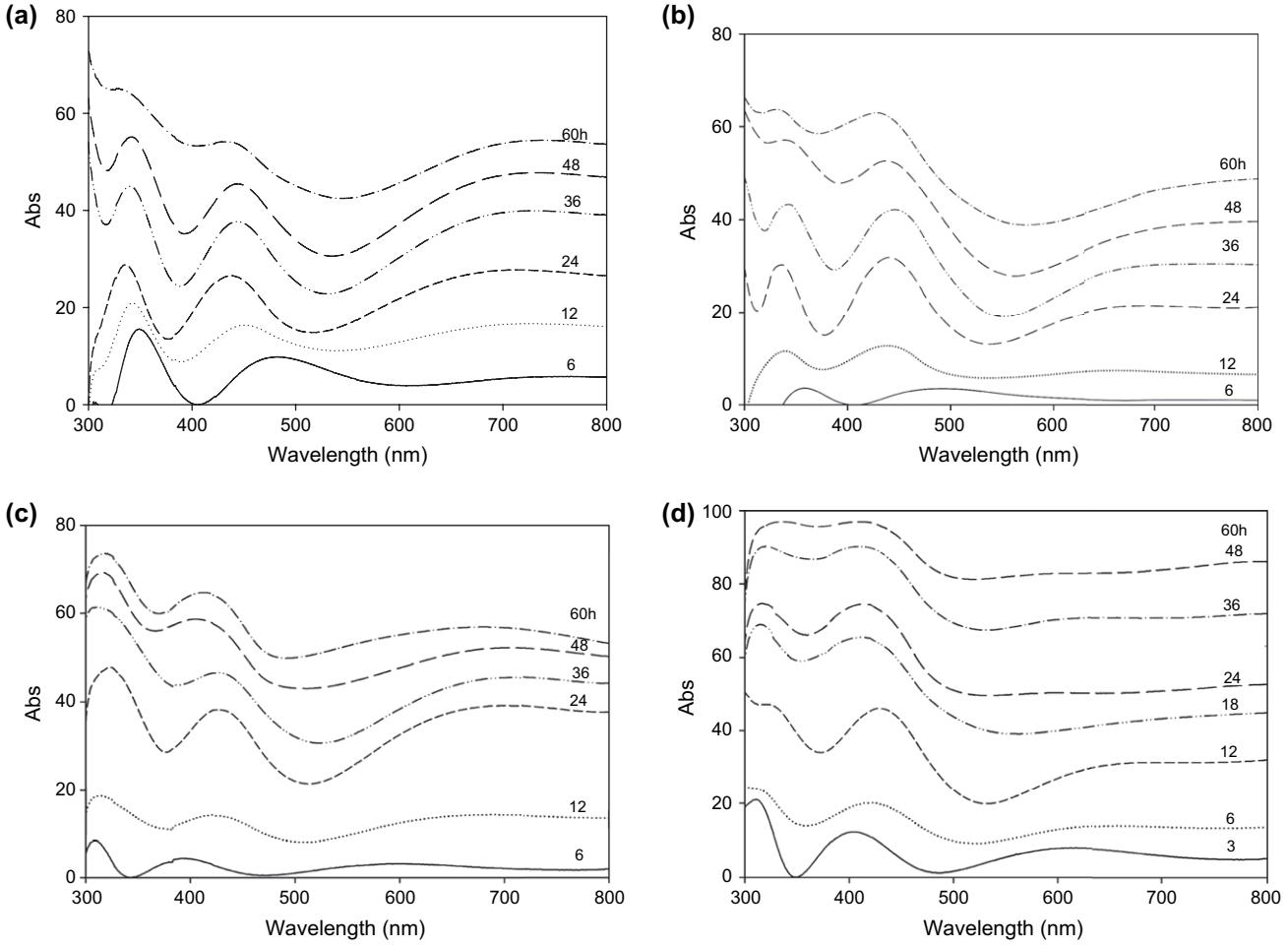

Fig. 3. UV–vis spectra of SPANI ultra-thin films self-assembled with AN/MSAN mole ratio of (a) 0.25 at 4 °C, (b) 1.0 at 4 °C, (c) 0.25 at 15 °C, and (d) 1.0 at 25 °C on ITO substrates at different assembly times.

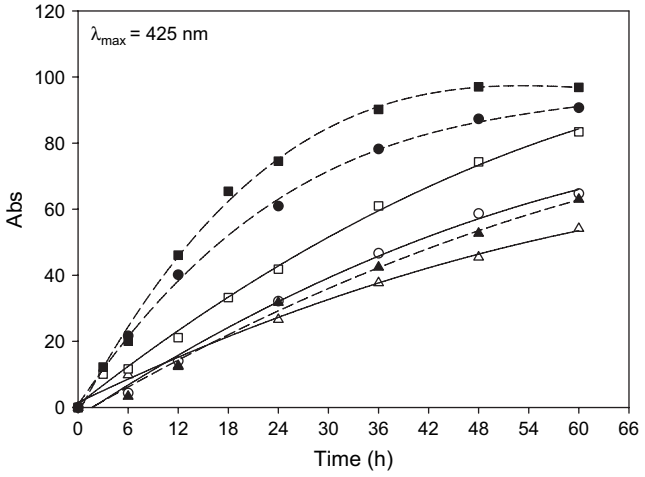

Fig. 4. The absorbance at $\lambda_{max} = 425$ nm from UV–vis spectra in Fig. 3 as a function of assembly time. Black and blank symbols represent the AN/MSAN ratio of 1.0 and 0.25, respectively. Symbols: (triangle) 4 °C, (circle) 15 °C, and (square) 25 °C.

increasing temperature, indicating that SPANI polymerization and deposition rates are enhanced with the increase of temperature. This reflects that copolymer formation improves the deposition (adsorption) rate of molecules. It is obvious that the deposition rate of AN/MSAN = 1 is higher than that of AN/MSAN = 0.25. This implies that the reactants of lower MSAN concentration have higher negative charges (lone pair electrons) readily adsorbing onto a charge substrate (ITO) through the formation of hydrogen bonding.

A series of cyclic voltammograms (CVs) of SPANI films on an ITO substrate in 0.1 M $LiClO_4$ propylene carbonate are shown in Fig. 5, revealing that the shape of these CVs is very similar to that of pure polyaniline [17–19]. In anodic sweep, the major redox couples appear at about 300 mV corresponding to the polymer form transition from emeraldine to radical cations. In the cathodic sweep, the corresponding broad reduction peak is presented. In Fig. 6, the values of i_p (from Fig. 5) increase with increasing assembly time and reaction temperature, indicating that the deposition of SPANI film increases with increasing the assembly time and reaction temperature. It is noteworthy that the potential of this peak shifts to higher potentials in longer assembly time. This shift is attributed to the presence of oligomeric species adsorbed on the ITO surface [17,18]. These oligomeric species are further polymerized in progress.

In this work, the α-step instrument is conveniently employed to measure the thickness of film (Fig. 7(a)). There exists a similar tendency between film thickness (Fig. 7(b)) and UV–vis absorbance at $\lambda_{max} = 425$ nm (Fig. 4) results. Also, the thickness of deposited SPANI films on the ITO electrode is directly proportional to the first anodic peak current density (i_p) (from CVs in Fig. 5). Approximately constant slopes on these lines indicate that the deposition rate of SPANI almost remains constant within the thickness of 60 nm. This result is very similar to that of AN/OSAN (*o*-aminobenzene sulfonic acid) system. But the deposition rate of AN/OSAN system is generally higher than that of AN/MSAN system.

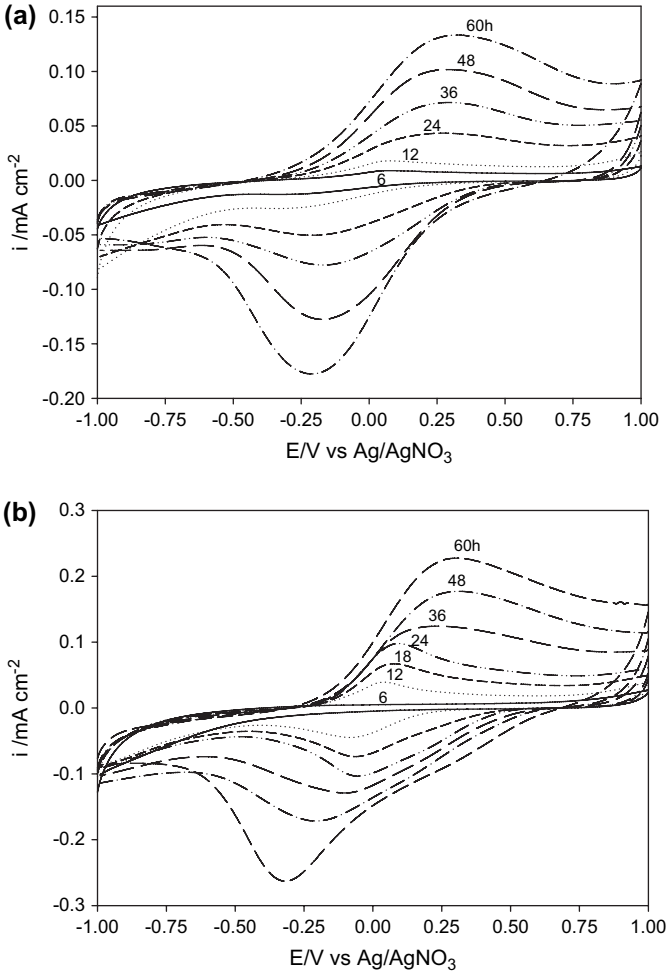

Fig. 5. Cyclic voltammograms of SPANI films on an ITO substrate in 0.1 M $LiClO_4$ propylene carbonate at a scan rate of 50 mV s^{-1}. SPANI films self-assembled at 4 °C with the AN/MSAN ratio of (a) 0.25 and (b) 1.0.

This might be related to the difference of molecular architectures between OSAN and MSAN. The correlations among film thickness, UV–vis absorption at $\lambda_{max} = 425$ nm, and the first anodic peak current density of CVs are presented in Fig. 8.

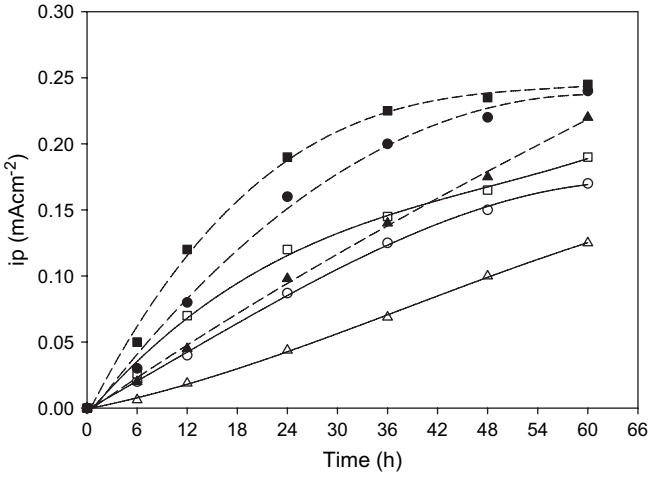

Fig. 6. The peak current density (i_p) from CVs in Fig. 5 as a function of assembly time. Symbols are the same as in Fig. 4.

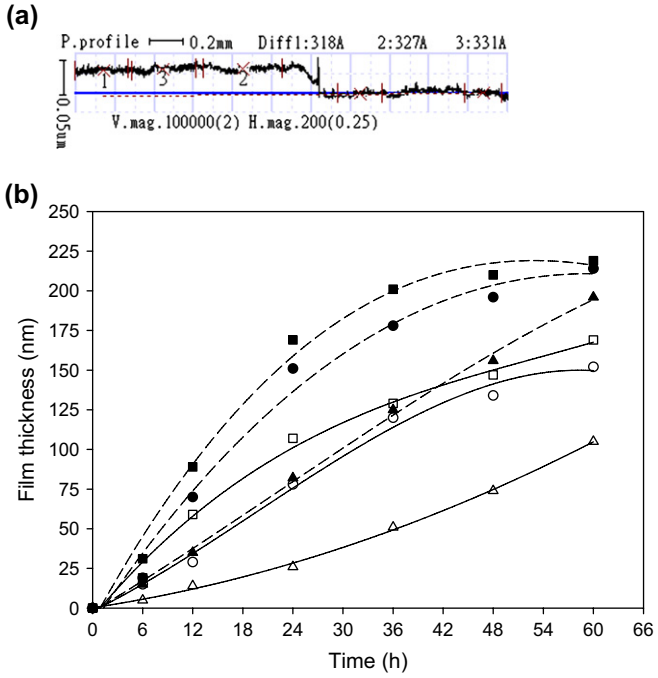

Fig. 7. (a) α-Step measurement of SPANI film thickness with AN/MSAN ratio of 0.25 assembled at 4 °C for 24 h and (b) plot of film thickness of SPANI versus assembly time. Symbols are the same as in Fig. 4.

Notably, such a positive correlation occurs between i_p and film thickness as well as between UV–vis absorption at $\lambda_{max} =$ 425 nm and film thickness in each case. These results reflect that it is convenient to measure the film thickness by monitoring UV–vis spectroscopy or recording CVs on the depositing SPANI films. A compositional depth profile for this SPANI film with AN/MSAN = 0.25 (24 h assembly time) in Fig. 9 shows C, N, S, O, In, and Sn trends. C, N, and S essentially

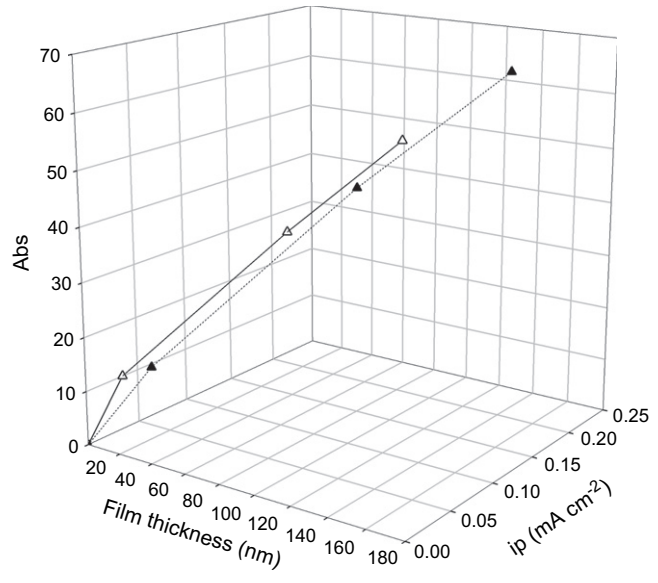

Fig. 8. Relationship between film thickness of SPANI and current density of the major anodic peak (from CVs in Fig. 5) as well as absorbance at $\lambda_{max} = 425$ nm (from UV–vis spectra in Fig. 3). Black and blank symbols represent the AN/MSAN ratio of 1.0 and 0.25, respectively.

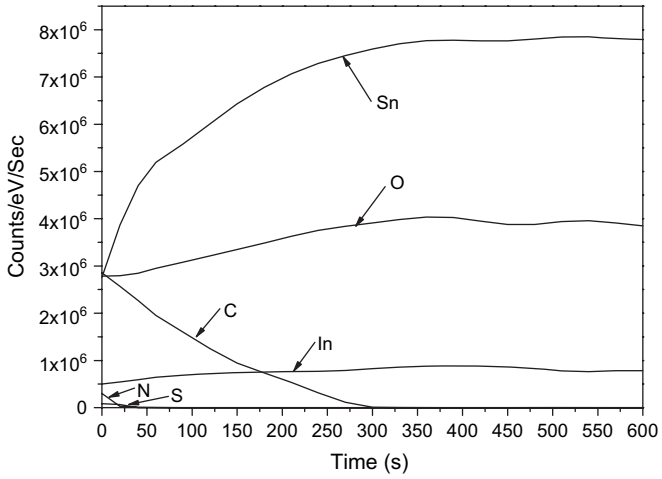

Fig. 9. Depth profile of elements in SPANI films with the AN/MSAN ratio of 0.25 assembled at 4 °C for 24 h.

exhibit a decline distribution in the bulk polymer film, whereas the N line is above S line arising from a co-deposition/copolymerization of AN and MSAN contents during the self-assembly. It is noteworthy that the declining slope of the N line is sharper than that of the S line; this result lends support to the supposition that the reactivity of AN is higher than that of MSAN in the deposition/copolymerization course. In, Sn, and O increase from the free surface to the substrate side, which exhibits a reasonable result of an ITO electrode. Also, this thickness result (ca. 30 nm) of SPANI film is very close to that measured by the α-step method (34 nm). Other compositional films have similar results. In Fig. 10(a), smooth ultra-thin films were readily obtained at lower reaction temperatures. In contrast, higher temperatures will lead to rough and cracked films (Fig. 10(b)), because the high polymerization/adsorption rate significantly results in a random architecture of deposition molecules (propagating polymers) at higher temperature. On the other hand, the lower ratio of AN/MSAN yields a more flat film (Fig. 10(a)) relative to the higher ratio of AN/MSAN (Fig. 10(c)). This arises from the fact that the higher AN/MSAN has a higher deposition rate, leading to a local aggregation of polymer chains.

Wide scanning provides a determination of which elements were present in an SPANI sample. The typical XPS survey scan of the SPANI (with AN/SAN ratio of 0.25) reveals that C, N, O, and S signals are detected in this polymer sample. The relative concentrations of C, N, O, and S in the polymer were calculated from the corresponding photoelectron peak areas after sensitivity factor corrections (SF = 1.00, 1.77, 2.14, and 2.85 for C_{1s}, N_{1s}, S_{2p}, and O_{1s}, respectively). The N_{1s} core-level spectra of the SPANI films have been deconvoluted by assigning binding energies of 399.1, 400.1, and 402.0 eV for the imine (−N═), amine (−NH−), and polaron species (N^+), respectively [19], as illustrated by the spectra in Fig. 11. Note that the second component peak (amine site) is dominant in the N_{1s} core-level spectrum of these SPANIs. The formation of N^+ (polaron site) is due to the nitrogen in the vicinity of H^+ cations when the polymers were self-doped with $-SO_3H$ groups (bearing on the polymer chain). On the

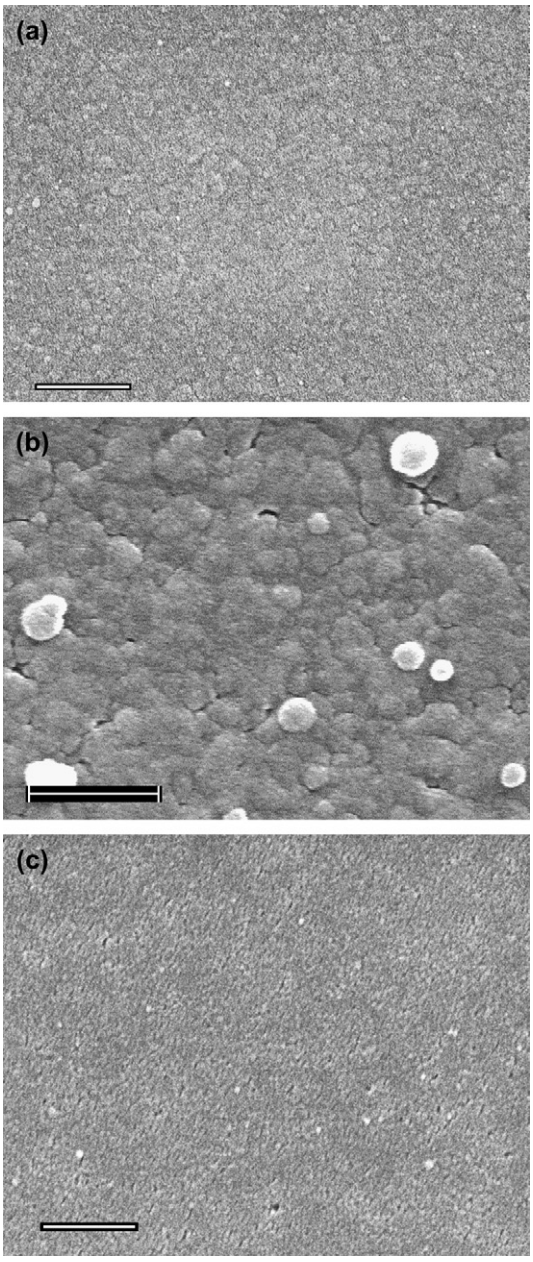

Fig. 10. FE-SEM image of SPANI films assembled with the AN/MSAN ratio of 0.25 at (a) 4 °C, (b) 25 °C, and (c) AN/MSAN = 1.0 at 4 °C for 24 h. Scale bar is 1 μm.

other hand, the imine site arises from the strong hydrogen bonding of −NH to oxygen atoms. The degree of doping, defined as $[N^+]/[N]$ (%), is shown in Fig. 12 revealing that the degree of doping increases with increasing MSAN concentration. It is reasonable that the concentration of H^+ cations increases with increasing $-SO_3H$ content. This increase results in a higher probability of nitrogen attaching to the H^+ cations. This explanation is consistent with the content of sulfur on the polymer chain (see Fig. 12). Furthermore, the S/N ratio is lower than the feed ratio of MSAN in the comonomers, indicating that the polymerization/deposition rate of AN is faster than that of MSAN. Also note that the degree of doping is smaller than the value of the S/N ratio. This reflects that

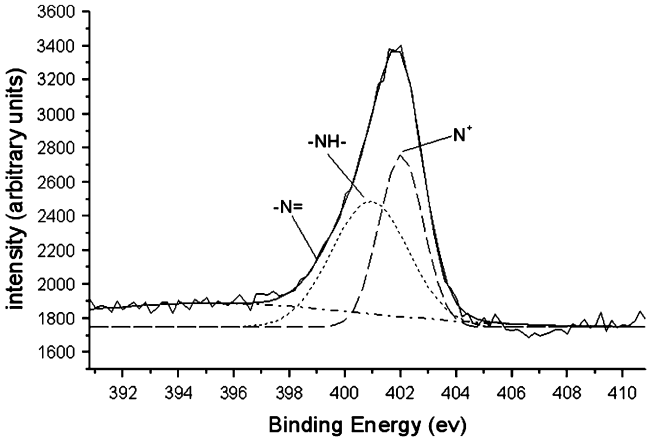

Fig. 11. XPS N_{1s} spectra of a SPANI film with AN/MSAN ratio of 0.25 assembled at 4 °C for 60 h. Dashed lines are the results of deconvolution.

the $-SO_3H$ groups are not completely used to dope the nitrogen atoms on the polymer chain. As compared SPANI films with AN/MSAN ratio of 0.25, the effect of temperature on both S/N value and degree of doping is insignificant for SPANI films with AN/MSAN ratio of 1.0.

3.2. Electrochromic properties of SPANI films

Fig. 13 exemplifies the results of spectrochronoamperometric studies, current variation (current density versus time), and optical response (absorbance versus time at $\lambda_{max} = 632$ nm), on a SPANI film (204 nm) with AN/MSAN ratio of 0.25. The Columbic efficiency, η, values of SPANI films (determined by the ratio of oxidation to reduction charges (Q_o/Q_c)) are presented in Table 1. The double (oxidation−reduction) potential steps were recorded and typical results are also listed in Table 1. The charge for the anodic process (Q_o) was found to be higher than that for the reduction process (Q_c). This can be explained as that total oxidized states were not completely reduced upon sweeping the potential back to 0.0 V. Consequently, a portion of the oxidized state would be presented

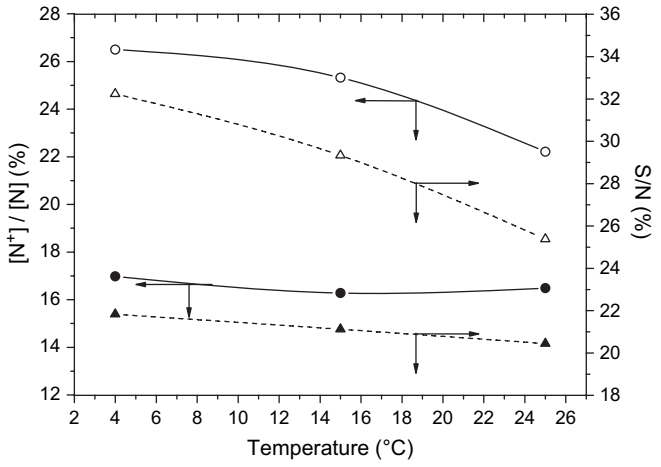

Fig. 12. Effects of AN/MSAN mole ratio and temperature on the doping degree (N^+/N (%)) and S/N value of SPANI films.

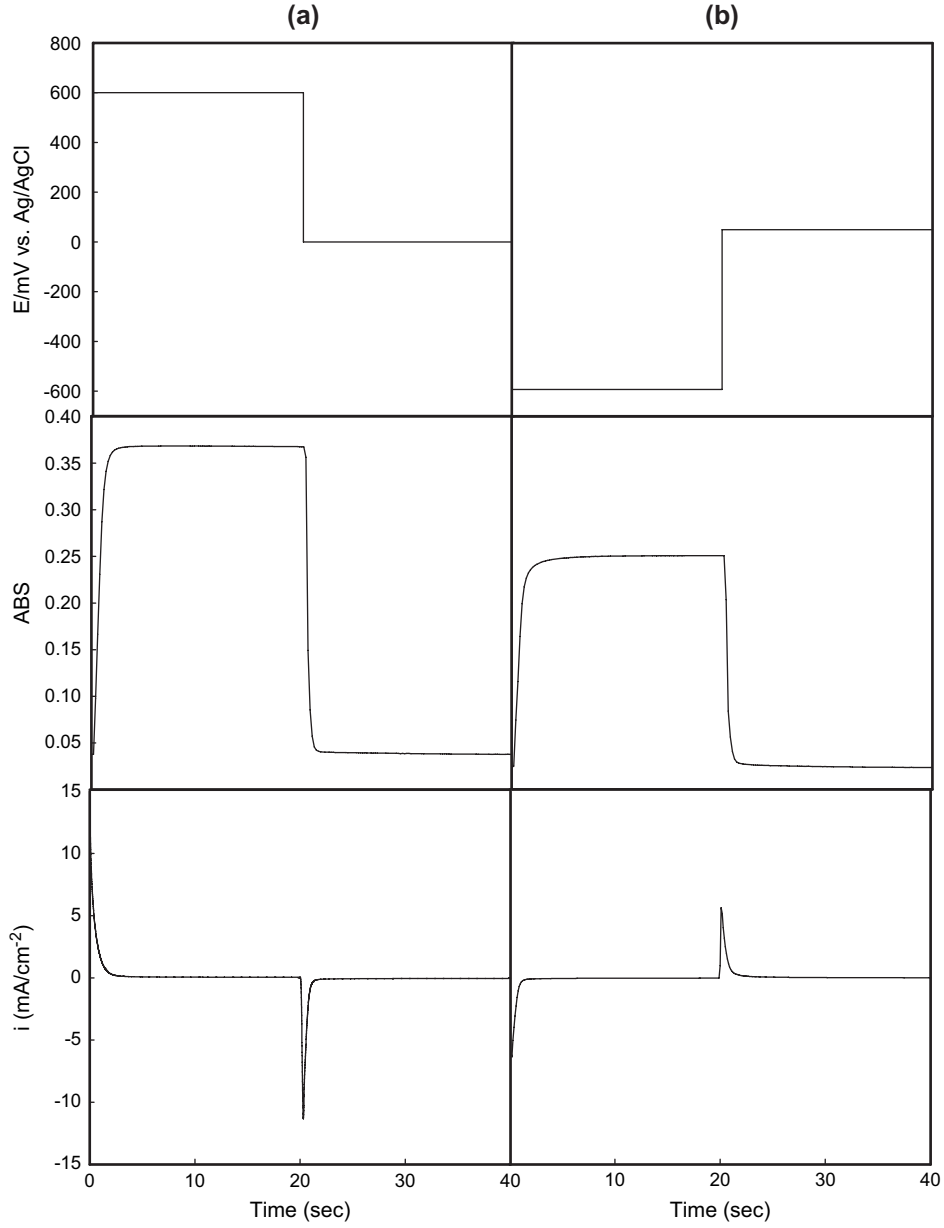

Fig. 13. Chronoamperometry (a) SPANI film at $\lambda = 632$ nm ranging from 600 to 0 mV and (b) PEDOT–PSS coated ITO at $\lambda = 630$ nm ranging from −600 to 0 mV, in a 1 M $HClO_4$ aqueous solution.

Table 1
Electrochromic properties of various SPANI films as determined by spectrochronoamperometry

SPANI film with AN/MSAN ratio (thickness)	Number of step	Q_o (mC cm^{-2})	Q_c (mC cm^{-2})	η (%)	T_c	T_b	ΔT	EE_c	EE_b
1.00 (204 nm) assembled at 4 °C	1	6.02	5.40	111.50	48.01	83.35	35.34	6.54	5.87
	100	4.39	3.98	110.30	58.12	92.21	34.09	8.56	7.76
0.25 (198 nm) assembled at 4 °C	1	5.67	5.16	109.88	54.20	91.43	37.23	7.21	6.56
	100	4.15	3.88	106.95	60.17	94.70	34.53	8.89	8.32
1.00 (201 nm) assembled at 25 °C	1	5.87	5.29	110.96	54.01	86.37	32.36	6.11	5.51
	100	4.31	3.92	109.82	59.30	91.21	31.91	8.14	7.40
0.25 (193 nm) assembled at 25 °C	1	5.28	4.65	113.53	58.21	91.34	33.13	7.12	6.27
	100	3.96	3.62	109.39	61.24	92.50	31.26	8.63	7.89

as residual oxidation state. The Columbic efficiency (η) of SPANI film at the first step is higher than that at the 100th step, indicating that the residual oxidation state is significant in the first step. The optical contrast value ($\Delta T\%$) is calculated from the difference between maximum transmittances at the coloration (T_c) and bleaching (T_b) states, revealing that the optical contrast of SPANI film in the first step is higher than in later steps.

The electrochromic efficiency (EE) was calculated from the ratio of optical contrast to charge density used for coloration/discoloration of polymer film. The variations in EE for coloration (EE_c) and bleaching (EE_b) with potential steps arise from the differences in redox charge. An examination of these data reveals that bleaching efficiency is always lower than coloring efficiency. Thus, the incomplete reduction of these polymers from its fully oxidized state causes variations in electrochromic properties of the polymer. The above observation indicates that a definite proportion of the oxidized state would undergo reduction and cause reproducible coloring–bleaching inter-conversions.

3.3. Solid-state electrochromic device

SPANI film was tried to assemble an electrochromic device. Before assembling the device, it is necessary to equilibrate the charge of SPANI and PEDOT:PSS modified electrodes to improve optical stability during repetitive charge/discharge processes. Therefore, these modified electrodes need to estimate the oxidation, Q_o, and reduction charges, Q_c, of each film material (see above section). Referring to Fig. 13, the values of Q_o and Q_c charges were obtained for the PEDOT:PSS films, ca. 1.4 and 2.5 mC cm^{-2}, respectively.

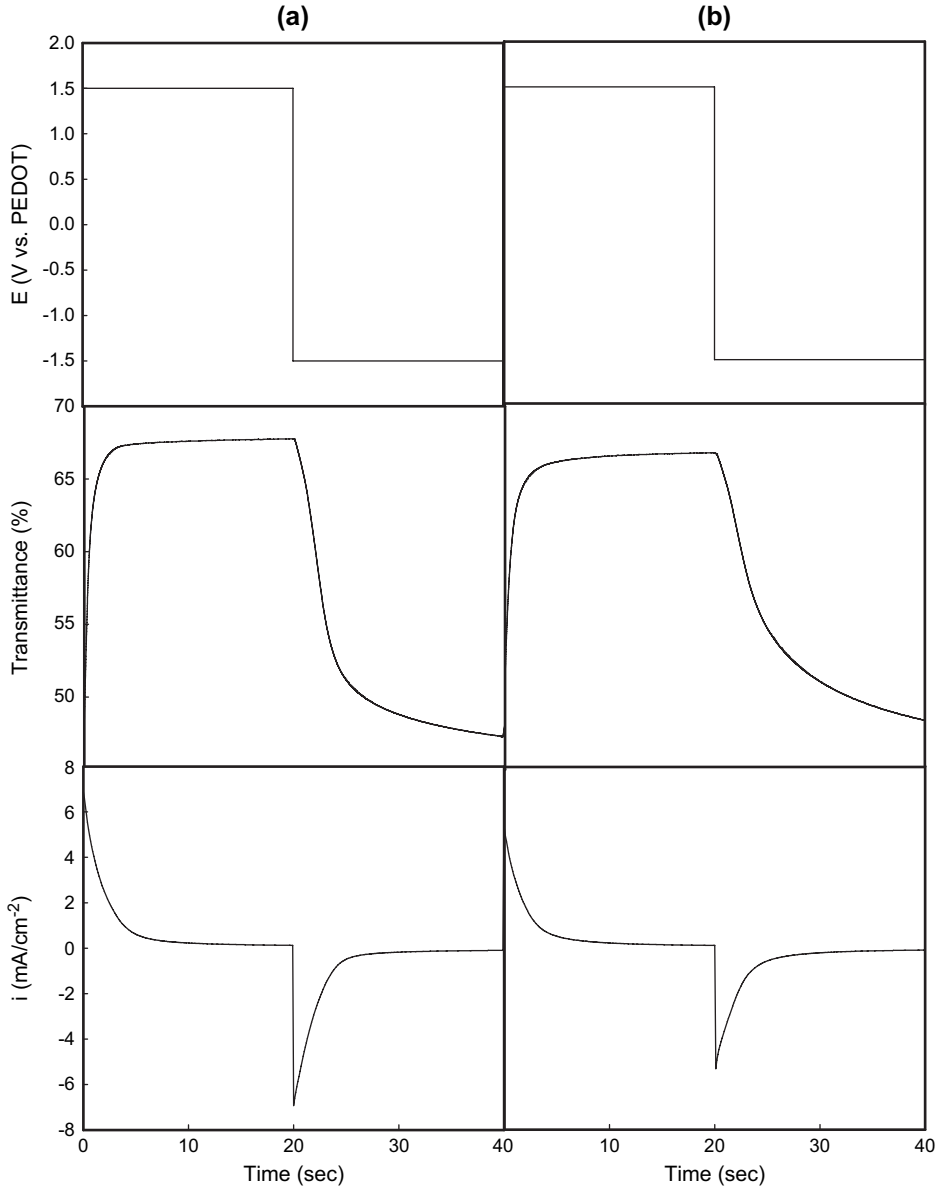

Fig. 14. Transmittance variation at $\lambda = 632$ nm, and current response for the device using SPANI (AN/MSAN mole ratio of 0.25 at 25 °C) coupled with PEDOT–PSS film during double-potential-step chronoamperometry ($E_1 = +1.5$ V, $E_2 = -1.5$ V and $t_{step} = 10$ s). (a) First and (b) 200th cycle.

Table 2
Electrochromic properties of the device at wavelength of the highest optical contrast ($\lambda_{max} = 632$ nm)

SPANI film with AN/MSAN ratio (thickness)	Temperature of film assembly	Switching cycle	ΔT (%)	τ/s (blue form)	τ/s (gray form)	η (%)
1.00 (204 nm)	4 °C	1	22.35	1.5	7.3	98.84
		200	15.21	3.3	9.6	95.69
0.25 (198 nm)	4 °C	1	21.68	1.3	5.7	104.82
		200	18.35	2.0	6.3	98.87
1.00 (201 nm)	25 °C	1	21.35	1.6	7.5	97.84
		200	14.15	3.4	9.8	97.14
0.25 (193 nm)	25 °C	1	21.07	1.4	6.2	105.74
		200	16.51	2.2	7.5	98.97

The electrochromic behavior of PEDOT:PSS has been confirmed by other authors [20]. The device ITO/SPANI (~200 nm)/CTBN/$LiClO_4$ (20 μm)/PEDOT:PSS (~200 nm)/ITO was assembled using transparent ITO electrodes coated with a SPANI film and a PEDOT:PSS film. Transmittance spectra recorded at −1.5 and +1.5 V give the highest optical contrast of ca. 22% (at $\lambda_{max} = 632$ nm) for the device. A double-potential-step chronoamperometry was performed to estimate the respective time of the device and its stability during consecutive scans. Potentials were stepped between −1.5 and +1.5 V with a cycle time of 20 s. The optical contrast (22%) was observed at $\lambda_{max} = 632$ nm. Fig. 14 demonstrates current–time and transmittance–time profiles for the device at the first and 200th cycles. The current decay reached zero after 10 s in the coloring process, while the decay to zero current was only 5 s in the bleaching process. This result reflects the faster de-doping of $SPANI^+ClO_4^-$ and deinsertion of Li^+ ion from PEDOT. Values of transmittance variation were simultaneously recorded at the wavelength of highest optical contrast. Table 2 summarizes the results obtained for the devices in the first and 200th cycle of double-potential-step spectrochronoamperometry experiments. An examination of Table 2 reveals that the complete device was subjected to 200 charge/discharge cycles and found a similar trend for these SPANI films. The most stable optical contrast (ΔT) of the device, corresponding to SPANI film with AN/MSAN ratio of 0.25 at 4 °C, was stabilized from ca. 22 to 18%; the change of the color from gray to blue was visually perceptible. The ΔT values of AN/MSAN system are a little lower than those of AN/OSAN system about 4%.

During the spectrochronoamperometry experiments, the stabilization of blue form transmittance is shorter than that of gray form for SPANI film. This behavior suggests a faster response time for the reduction of SPANI/oxidation of PEDOT:PSS than for the reverse process due to the faster kinetics of dopant ion diffusion. Moreover, the response time is relatively short in the SPANI-based device. Also note that the current–time curve of the device using SPANI film with AN/MSAN mole ratio of 0.25 at 25 °C was practically unchanged after 200 double-potential-steps (refer to Fig. 14). The Columbic efficiency (η), calculated from the ratio between the coloring and the bleaching charge, was 105% in the first cycle and decreased to 99% in the 200th cycle, indicating that the doping/de-doping process of polymeric film needs a certain number of charge/discharge cycles to stabilize. This could be caused by the conformational changes occurring during their redox processes. Actually, the figure features of this double-potential-step experiment are very similar to those of 3-trimethoxysilanylpropyl-*N*-aniline-2,5-dimethoxyaniline (TMSPA-DMA)-based devices except the differences of demonstrated colors and device stability [21].

4. Conclusions

We have successfully integrated AN and MSAN into electrostatic self-assembled films, both with MSAN as a surfactant, a dopant, and a monomer, and with APS as oxidant performed copolymerization from a mixture of AN and MSAN aqueous solution. Moreover, we have demonstrated that self-assembly coupled with copolymerization can be used to accomplish this deposition scheme. Our results widen the range of applications for the self-assembly technique, which will become a popular method of ultra-thin film formation. Both factors of AN/MSAN ratio and reaction temperature significantly influenced the film formation behavior in the film deposition process. We found that using a high AN/MSAN ratio as a co-adsorbing agent can dramatically enhance the rate of film deposition and that a higher deposition rate occurs at higher reaction temperatures. In addition, different deposition rates exist for AN and MSAN when the two materials simultaneously copolymerize/adsorb from a common polymerization solution. Our results here demonstrate significant progress in attaining directed control of self-assembled copolymerization layers. A total solid electrochromic device was assembled with the configuration of ITO/SPANI/$LiClO_4$–CTBN/PEDOT:PSS/ITO. The device was found to have stable Columbic efficiency (~100%) and optical contrast (~20%). The device possesses perceptible color changes from gray to dark blue with switching potentials from −1.5 to 1.5 V.

Acknowledgment

Financial support from the National Science Council in Taiwan (NSC-95-2221-E-218-060 and NSC-95-2622-E-218-020-CC3) is gratefully acknowledged.

References

[1] McDiarmid AG. Synth Met 2002;125:11.
[2] Yang CH, Chih YK, Wu WC, Chen CH. Electrochem Solid-State Lett 2006;9(1):E5.
[3] Lakes R. Nature 1993;361:511.
[4] Kuhn H, Mobius D. Angew Chem Int Ed Engl 1971;10:620.
[5] Blodgett KB. J Am Chem Soc 1934;56:495.
[6] Netzer L, Sagiv J. J Am Chem Soc 1983;105:674.
[7] Cao G, Hong HG, Mallouk TE. Acc Chem Res 1992;25:420.
[8] Cassagneau T, Mallouk TE, Fendler JH. J Am Chem Soc 1998;120:7848.
[9] Decher G. Science 1997;277:1232.
[10] Laurent D, Schlenoff JB. Langmuir 1997;13:1552.
[11] Campbell VE, Chiarelli PA, Kaur S, Johal MS. Chem Mater 2005;17:186.
[12] Ho PKH, Kim JS, Burroughes JH, Becker H, Li SF, Yu H, et al. Nature 2000;404:481.
[13] Stuart MAC, Fleer GJ, Lyklema J, Norde W, Scheutjens JMHM. Adv Colloid Interface Sci 1991;34:477.
[14] Yang CH, Chih YK, Cheng HE, Chen CH. Polymer 2005;46:10688.
[15] Besbes S, Ltaief A, Reybier K, Ponsonnet L, Jaffrezic N, Davenas J, et al. Synth Met 2003;138:197.
[16] Shipway AN, Katz E, Willner I. ChemPhysChem 2000;1:18.
[17] Yang CH, Wen TC. J Electrochem Soc 1994;141:2624.
[18] Yang CH, Wen TC. J Electrochem Soc 1997;144:2078.
[19] Yue J, Epstein AJ. Macromolecules 1991;24:4441.
[20] Carlberg JC, Inganas O. J Electrochem Soc 1998;145:3810.
[21] Yang CH, Liu SJ, Chang CC, Lin LY. J Electroanal Chem 2006;590:161.